Appl. Phys. B (2017) 123:222
DOI 10.1007/s00340-017-6793-9

Applied Physics B
Lasers and Optics

Sub-wavelength resolution dynamics of semiconductor passively mode-locked lasers induced by optical feedback

Christos Simos[1,2] · **Hercules Simos**[3,2] · **Dimitris Syvridis**[2]

Received: 19 November 2016 / Accepted: 11 July 2017 / Published online: 28 July 2017

Abstract We present a numerical analysis that focuses, for the first time to our knowledge, on the feedback-induced dynamics in a semiconductor passively mode-locked laser with sub-wavelength resolution. Our results and the corresponding theoretical explanations elucidate several aspects of the laser dynamics under self-injection including inherent properties of mode-locked lasers such as pulse intensity noise and timing jitter. We show that the dynamics of the laser exhibit a periodicity in the wavelength scale apparent only on integer multiples of the laser cavity and decays in the time scale of the pulse duration following the coherence of the mode-locked laser. The corresponding phenomena are dominant for external cavities that are shorter than the laser cavity and superimposed on the previously reported dynamics of the semiconductor mode-locked lasers for longer external delays. Since these dynamics are triggered by low feedback levels, our study could be useful for the optimization of the laser operation in cases where ultra-short external cavity lengths are involved (integrated designs, power collection with fiber tapers, etc.).

✉ Christos Simos
christos.simos@teiste.gr

[1] Department of Electronic Engineering TE, Technological Educational Institute of Sterea Ellada, 35100 Lamia, Greece

[2] Department of Informatics and Telecommunications, Optical Communications Laboratory, National and Kapodistrian University of Athens, 15784 Athens, Greece

[3] Department of Electronic Engineering TE, Piraeus University of Applied Sciences, 12244 Athens, Greece

1 Introduction

Optical feedback has been found to have an important impact on the operation of semiconductor passively mode-locked lasers (MLLs). In general, MLLs exhibit different dynamics under feedback than their continuous wave (CW) counterparts due to their inherent multimode nature as well as the presence of the saturable absorber which imposes the phase locking between the longitudinal modes. Several previous theoretical and experimental works have investigated the dynamics of quantum well or quantum dot MLLs under self-injection of short, intermediate or long delays. In the literature, the classification of the optical feedback time scale is usually based on the characteristic frequencies of the system and the corresponding lengths. A short delay feedback system is defined when the characteristic frequency of the external cavity (f_{ext}) is higher than the relaxation oscillation frequency of the free running laser (f_{ro}), or equivalently when the distance to the external reflector (L_{ext}) is lower than the corresponding relaxation oscillation length (L_{ro}) [1]. Furthermore, the ultra-short delay feedback regime is defined when the length of the external cavity is lower than the length of the laser cavity (L_{las}) and in this case the mode separation of the internal cavity becomes shorter than that of the external cavity [2].

For intermediate and long external cavity lengths, it has been found that in the majority of cases a relatively reasonable feedback level enhances the temporal characteristics of the semiconductor mode-locked lasers that is, decreases timing jitter and the related intensity noise and stabilizes the repetition rate [3–7]. The laser dynamics for this scale of feedback delays is dominated by the repetition rate pulling effect, which is manifested as a periodic sawtooth-like dependence of the repetition rate of the laser on the external cavity length [5, 6, 8]. The period of the

phenomenon equals the laser cavity length while the difference between the maximum and minimum values of the repetition rate equals the external cavity mode spacing. In this case, the external cavity length imposes the repetition rate of the laser to be an exact multiple of its characteristic frequency. Therefore, feedback and laser pulses are always synchronized which explains the findings of simulations and experiments related to increased performance of the laser in terms of phase and intensity noise.

The short external cavity case has been found to have a rich dynamics as well [7, 9, 10]. Here, the pulling effect is present as well but it is weaker and incomplete compared to the long cavity case due to the long spacing between the external cavity modes [7]. The timing characteristics of the laser have been found enhanced for integer cavity ratios (resonant case), whereas harmonic mode locking or mode locking collapse has been demonstrated, respectively, for fractional or irrational cavity ratios [9, 10].

All the above works study feedback-induced phenomena that exhibit a microwave scale periodicity which is related to the pulse repetition rate (the periodicity is equal to the laser cavity length). Therefore, in simulations and experiments only macroscopic changes of the external cavity have been considered, usually in submultiples of the laser cavity whereas smaller scale dynamics are ignored. Nevertheless, numerous studies for CW semiconductor lasers have shown that rich dynamics occur in a sub-wavelength scale when the external delay is within the laser coherence (a brief review can be found in [2]). However, no such information for semiconductor MLLs has been reported. The present work is the first study to our knowledge which investigates with a sub-wavelength resolution the dynamics of semiconductor MLLs induced by self-injection. In particular, by means of a detailed numerical analysis and the corresponding theoretical explanations, we elucidate the impact of optical feedback on the inherent characteristics of semiconductor MLLs such as optical power, repetition rate, pulse intensity noise and timing jitter considering sub-wavelength changes of the external cavity. We focus our study on the ultra-short delay case (an analysis for CW lasers has been reported in [11, 12]) and extend our results to longer delays considering the impact of the coherence characteristics of MLLs. The results presented in this work can be particularly useful for the optimization of the mode-locking operation in all cases where ultra-short external cavity lengths are involved such as in fiber-based power coupling applications as well as in integrated designs.

2 Model details

Simulations presented in this paper have been performed with a delayed differential equation (DDE) numerical model for MLLs [6]. This model assumes a unidirectional ring cavity approximation for a quantum dot laser and was fine-tuned to achieve quantitatively matching results with a more accurate time domain traveling wave model, while maintaining its main advantage of being significantly faster. The model includes spontaneous emission noise and feedback terms to simulate the external cavity. Since the analysis presented in the following sections is not based on the particular dynamics of quantum dot lasers, we assume that the results are valid for any similar semiconductor MLL. Full model details and laser fundamental parameters are given in [6]; here we just review what is absolutely important for the comprehension of the paper. We consider a two-section (gain and absorber) unidirectional ring laser with a (cold) cavity length equal to $L_{\mathrm{las}} = 4$ mm, emitting from the ground state at 1252 nm. Cavity refraction index for the ground state wavelength is 3.34. This configuration corresponds to a Fabry–Perot laser of 2 mm. With a forward current of 250 mA and an absorber voltage of −5.5 Volts the laser emits mode-locked pulses of ~5 ps duration at a repetition rate of approximately 22.2 GHz in free running state. The linewidth enhancement factor α of the laser is considered equal to 1, otherwise it is explicitly mentioned.

3 Results and discussion

Figure 1 shows the laser average power, repetition rate and amplitude noise of the output pulse trains versus the external cavity length which varies around a macroscopic value of 50 μm with ~30 nm step, assuming a feedback level of −40 dB. We realize that the dynamics of the laser exhibit a variation with a periodicity of λ, where $\lambda = \lambda_0/n = 375$ nm is the wavelength in the external cavity of refractive index $n = 3.34$. Taking into account that in the simulation we use a ring laser, this periodicity corresponds to the well-known $\lambda/2$ condition of a Fabry–Perot cavity. The emitted average power oscillates around the free running value (black dashed line in Fig. 1), whereas the maximum and minimum values are obtained when the returning field is, respectively, in and out of phase, with the laser field on the output cavity mirror. This picture is reminiscent of the behavior of CW semiconductor lasers under self-injection when the mirror position varies in a sub-wavelength scale and has been attributed to the induced effective reflectivity due to the coupling on the output mirror of the reflected field with the field in the laser cavity [2]. This effective reflectivity of the output laser mirror depends sinusoidally on the external cavity round-trip phase. Since the gain in the laser cavity is a function of the reflectivity, in the presence of optical feedback the gain varies periodically with the change of the optical phase of the return field, which in turn induces a modulation on the emitted optical power. Furthermore,

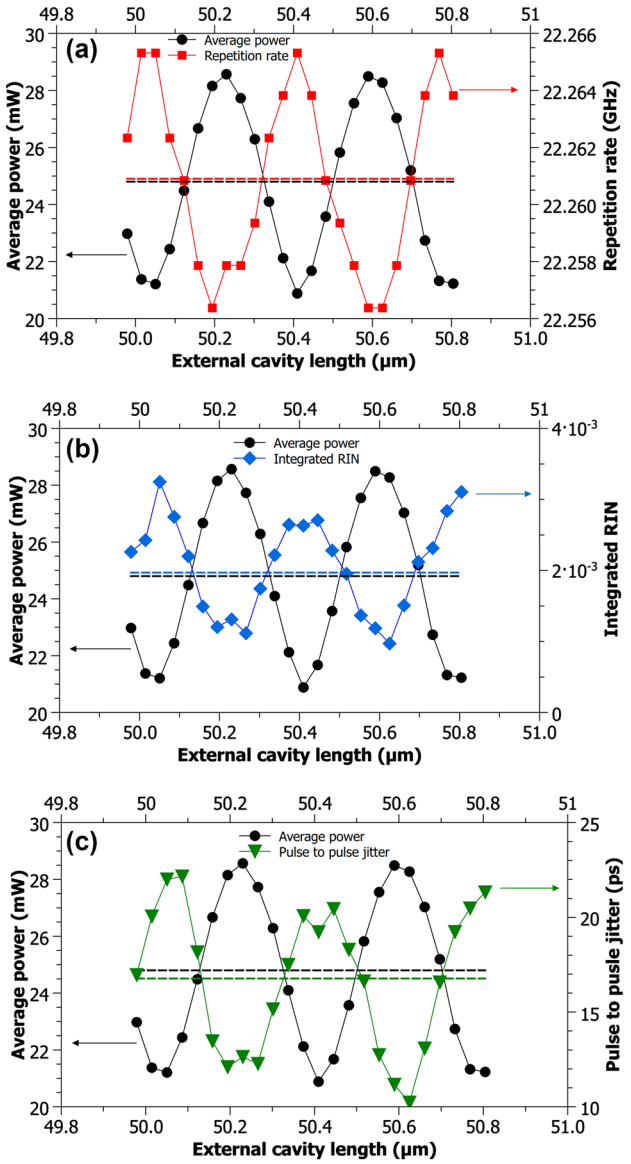

Fig. 1 **a** Average power and repetition rate, **b** average power and relative intensity noise, **c** average power and pulse to pulse jitter versus the external cavity length for nanometric fine tuning around a macroscopic value of approximately 50 μm. *Dashed lines* show the corresponding values for the free running laser

similarly to the average power, the repetition rate of the laser exhibits as well a periodic variation of ~10 MHz in the wavelength scale (red curve in Fig. 1), most likely due to the corresponding change of the lasing conditions. This periodicity of the repetition rate is in very good agreement with the experimental findings of [13] for a passively MLL under feedback from a tapered fiber and suggests a different mechanism compared to the sawtooth-shaped dependence with a period equal to the cavity length [5–8] that occurs when macroscopic changes of the (longer) external cavity are considered.

Moreover, the amplitude noise of the pulses has been evaluated by calculating the relative intensity noise (RIN) spectrum of the output field [6] and integrating the baseband frequency range from 1 MHz to ~11 GHz. The upper frequency limit (11 GHz) is the half of the repetition frequency (~22 GHz) and corresponds to the Nyquist frequency since pulse peaks are used for the calculation, whereas the lower limit (1 MHz) is the reciprocal of the total duration of each time series (~1 μs). The integrated RIN versus the external cavity length is shown in Fig. 1b (blue curve) together with the optical power for reference. The RIN exhibits a similar periodic variation relative to the free running value (blue dashed line in Fig. 1b) being antiphase with the optical power variation. This behavior was theoretically predicted and experimentally observed for CW lasers under optical feedback in early works [14–16] and proposed as a method to reduce the phase and amplitude noise of the laser. The noise reduction was then explained within the context of the detuned loading effect proposed by Vahala et al. [17] and extended for different cases in [18]. In [18], the amplitude noise variation was considered as the result of a modified amplitude-phase coupling under the influence of an external cavity with frequency/phase dependent losses, which drives the laser to operate either in higher or in lower RIN levels than the free running value. Briefly, the amplitude fluctuations are transformed to phase noise through the intensity to phase coupling, thus generating a correlation between the amplitude noise and the instantaneous frequency. These perturbations of the output field are re-entering the laser cavity through the feedback path and drive the laser to change operation point depending on the optical phase of the external path. With this method, a reduction of amplitude noise was achieved in the case of CW lasers for frequencies lower than the characteristic frequency of the external cavities, with a maximum of $1/(1 + \alpha^2)$ and for operation near the threshold [16] (α is the linewidth enhancement factor). The relative intensity noise spectra for the maximum and the minimum RIN values of the oscillation are shown in Fig. 2 (red and blue curve, respectively). Besides RIN, the other significant factor which determines the stability and quality of the mode-locked operation is the timing jitter of the emitted pulses. This is a specific characteristic of MLLs with no sense in CW lasers, being directly related to the mode-locking procedure since it is associated with the operation of the saturable absorber. In a first time, we used the pulse to pulse jitter as the metric for timing stability calculated by averaging the ensemble of successive timing fluctuations of pulses in a single noise realization supposing uncorrelated timing fluctuations [19]. The variation of the pulse to pulse jitter versus the external cavity length is shown in Fig. 1c (green curve with triangular points) together with the optical power for reference (black curve with circular points).

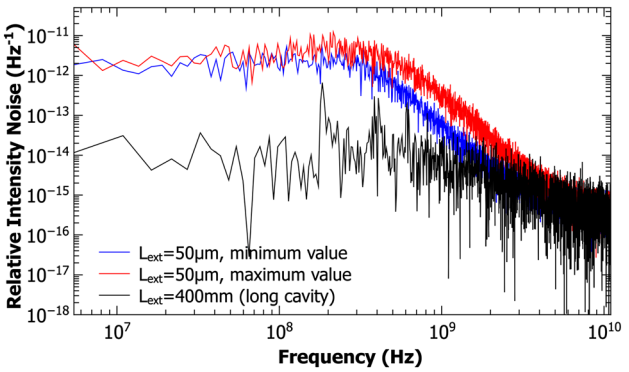

Fig. 2 RIN spectra corresponding to minimum (*blue line*) and maximum (*red line*) values of the integrated RIN of Fig. 1. *Black curve* shows the long cavity case as discussed in the analysis of Fig. 4

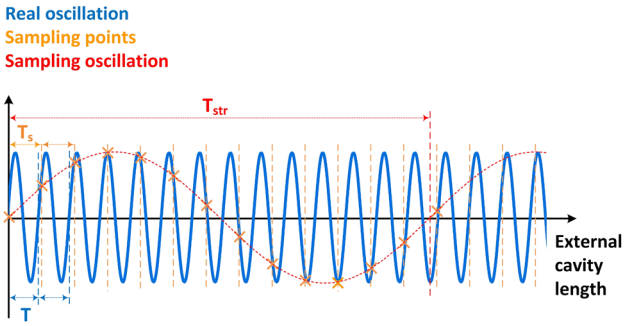

Fig. 3 Sketch of the stroboscopic technique used in simulations of Fig. 4 and afterwards to achieve practical simulation times

It is obvious that the integrated jitter follows the amplitude noise oscillation (Fig. 1b), most likely due to the coupling of the amplitude to the timing fluctuations in the operation of a slow saturable absorber as shown in various works [20, 21].

For all the above results, a time discretization (simulation step) as low as 0.4 fs was necessary to appropriately resolve the 30 nm external cavity increments. This resulted in impractically long simulation times and huge datasets since sufficiently long time traces had to be simulated in order to be sure that the laser arrives at a stabilized state. Therefore, using the above-mentioned parameters, it would be impossible to perform a complete numerical analysis of the phenomenon considering several impact parameters (longer cavities, feedback level, linewidth enhancement factor). For this reason, we performed our subsequent analysis based on the stroboscopic principle that is by taking snapshots at different phases of consecutive oscillatory cycles. By carefully selecting the stroboscopic frequency, we were able to use a time step as high as 8 fs which permitted to obtain 14 points per period. This method is sketched in Fig. 3 and was used to acquire all data of Fig. 4 and afterwards.

Fig. 4 Variation of the emitted average power, repetition rate, relative intensity noise and pulse to pulse jitter versus nanometric variations of the external cavity around the macroscopic values of 30, 50, 110, 225, 500 μm, respectively, from **a** to **e**. Feedback level is −40 dB. *Dashed* and *dotted lines* show the free running and the long cavity values, respectively

Figure 4 shows the simulated results for macroscopic cavities of approximately 30, 50, 110, 225 and 500 μm using the stroboscopic method. The 50 μm case permits to confirm the validity of the results obtained with the stroboscopic method since it gives identical results with the full step simulation of Fig. 1. From Fig. 4, we remark that with increasing external cavity the oscillations of power, repetition rate, RIN and jitter decrease and although they remain periodical, their sinusoidal form is progressively altered. This is most likely due to the combination of two co-existing phenomena. The first is the interference of the delayed and output fields on the laser output mirror which occurs within the coherence length of the mode-locked laser (the length that is reciprocal to the overall width of the optical spectrum or the length that corresponds to the time scale of the pulse duration). The second is specific to the mode-locking process, being related to the absorber operation and the RF frequency-pulling effect that occurs in a wide range of external cavity length assuming sufficient feedback strength. This is most likely the reason for the much stronger maximum reduction of RIN observed in our case (>20 dB around 110 μm) as compared to the $1/(1+\alpha^2)$ prediction for CW lasers (which would yield a 3 dB reduction, with $\alpha = 1$ in our case). As the external cavity reaches the limited coherence length, the oscillation due to the interference of the output with the delayed field fades and the RF frequency pulling establishes and progressively becomes dominant. The latter can be confirmed by the monotonically decreasing mean value of the repetition rate for increasing L_{ext} in each case of Fig. 4: [22.263, 22.260, 22.255, 22.220, 22.174] GHz. The linear slope of the repetition rate change with the external cavity length corresponds to a small part of the RF frequency-pulling function, typical for the MLLs under feedback in the short and long delay regimes [6, 7].

To validate the timing jitter calculations as well as to have a direct correlation to the RIN calculation method, we also evaluated the timing stability in terms of the integrated (rms) jitter, which was calculated by integrating the phase noise spectrum of the output pulses from 1 MHz to 11 GHz. The phase noise spectrum has been derived by means of a purely temporal method which uses the timing fluctuations of the pulses and the ensemble averaging over multiple noise realizations as presented in [22]. This method is more appropriate for passive MLLs than the von der Linde method [23] which proposes to measure the power spectral density of the phase noise from the power spectral density of the photocurrent

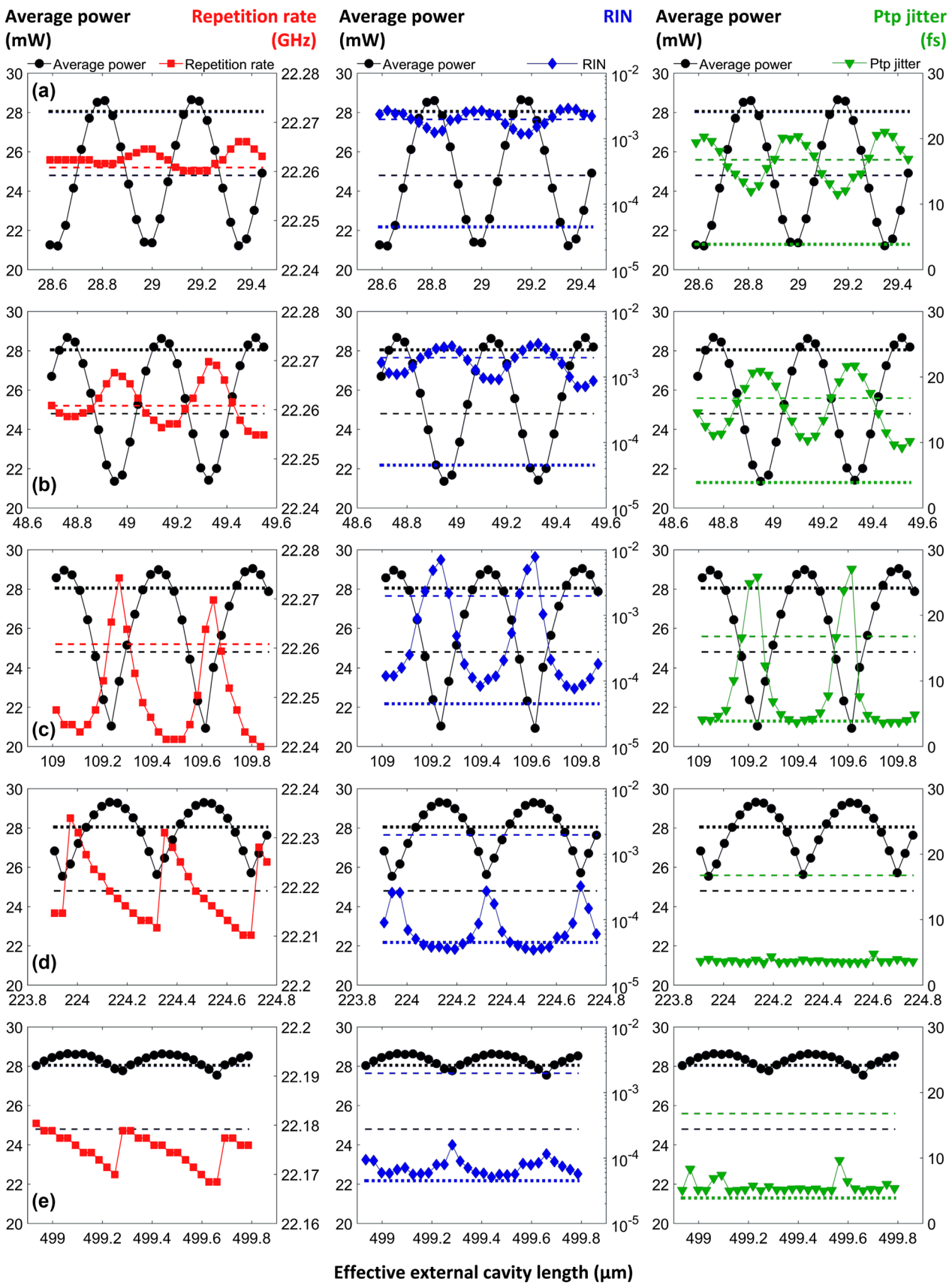
Average power (mW)
Repetition rate (GHz)
Average power
Repetition rate
RIN
Ptp jitter (fs)
(a)
(b)
(c)
(d)
(e)
Effective external cavity length (μm)

(that is the power spectrum), and can lead to serious underestimation of jitter in PMLLs due to the unbounded variance of their timing fluctuations as a result of the absence of external reference, which is analogous to what happens in random walk processes [3, 4, 24–26]. Figure 5a shows the integrated rms jitter versus the external cavity length together with the average optical power for reference for a specific case of Fig. 4 (around 49 μm), calculated from 20 statistically independent runs. Since the calculation of the integrated jitter requires impractically long calculation times due to the large number of noise realizations that are necessary to obtain a meaningful result, we could not perform complete comparison for a

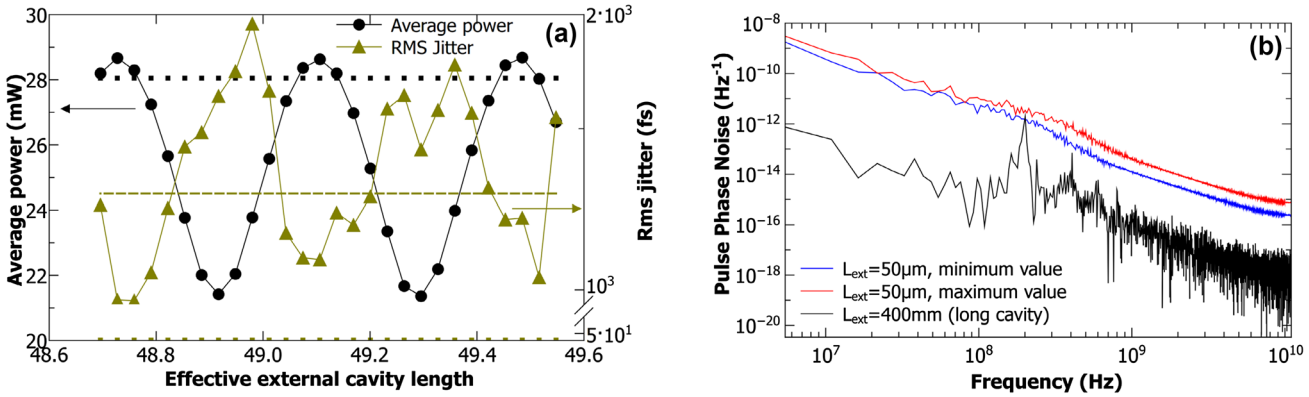

Fig. 5 **a** Average power and integrated rms jitter versus nanometric variations of the external cavity around a macroscopic length of 50 μm for a feedback level of −40 dB. *Dashed* and *dotted lines* show the free running and the long cavity values, respectively. **b** Pulse phase noise spectra corresponding to minimum (*blue line*) and maximum (*red line*) values of the integrated jitter of **a**. *Black curve* shows the spectrum of the long external cavity case

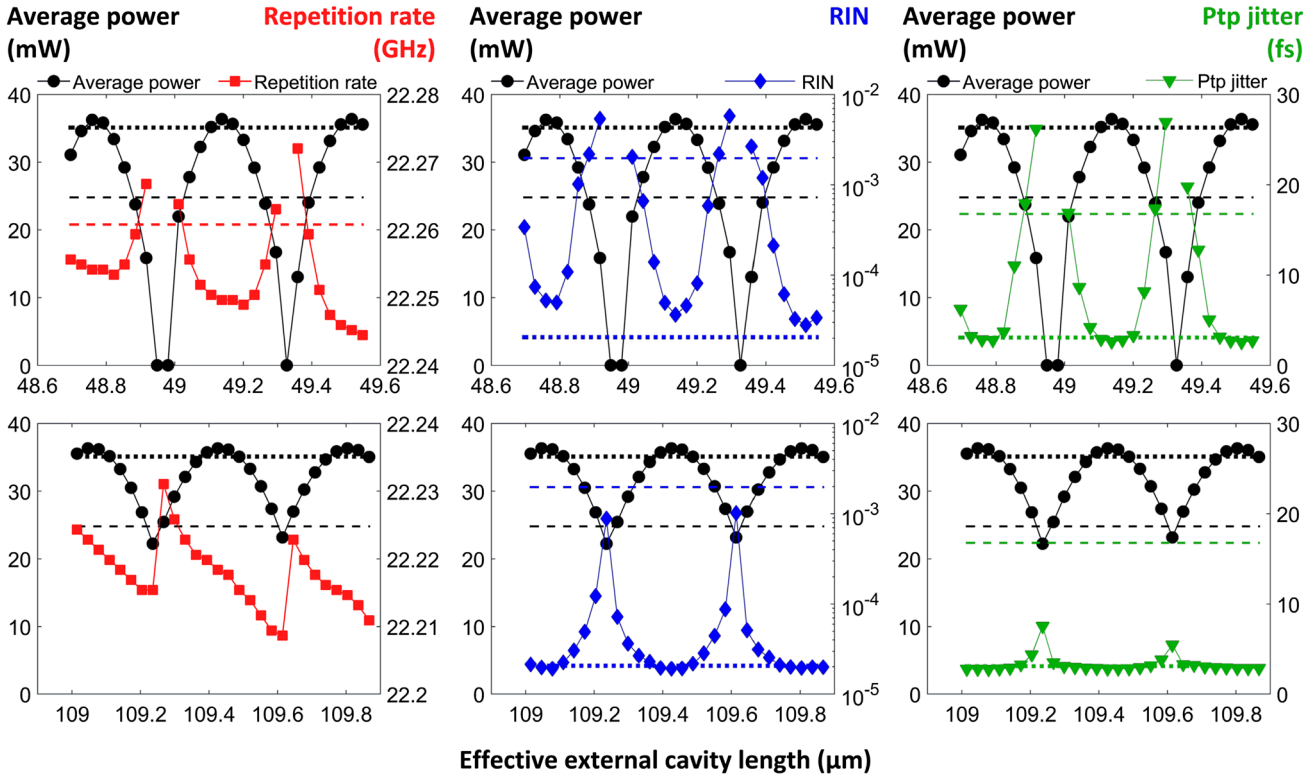

Fig. 6 Repetition rate (*left*), RIN (*center*) and pulse to pulse jitter (*right*) versus nanometric variations of the external cavity around the macroscopic values of 50 μm (*up*) and 110 μm (*bottom*) (corresponding to cases **b** and **c** of Fig. 4) for a feedback level of −30 dB. *Dashed* and *dotted lines* show, respectively, the free running and the long cavity values. *Missing points* denote that the laser exhibited only spontaneous emission. The evolution of average power is shown for reference in all graphs

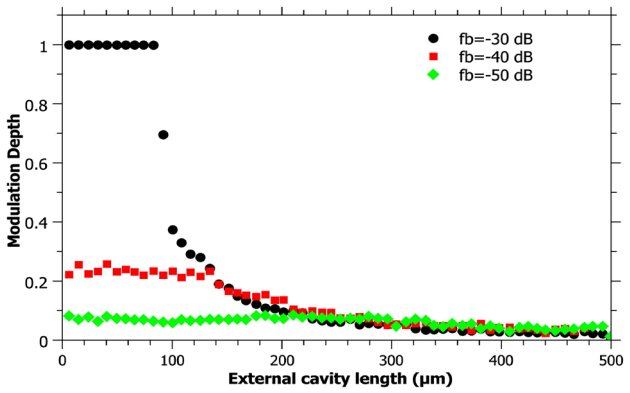

Fig. 7 Average power modulation depth versus the external cavity length for feedback levels −50, −40 and −30 dB

wide range of external cavity lengths but only a validation of the calculated timing fluctuation behavior. Although there is some uncertainty due to the relatively low number of averaged noise realizations, it is obvious that the integrated jitter exhibits the same periodic variation to the RIN and pulse to pulse jitter around its free running value (green dashed line in Fig. 5), signature of the coupling between amplitude and timing instabilities. The phase noise spectra for the maximum and minimum values of jitter oscillation are shown in Fig. 5b (red and blue curve, respectively).

Furthermore, in order to investigate the impact of feedback level to the decay of oscillations with increasing cavity length, we have plotted in Fig. 6 the evolution of the average power, repetition rate, RIN and pulse to pulse jitter for two characteristic external cavity lengths corresponding to the cases (b) and (c) of Fig. 4. What is important to retain from Fig. 6 is that the oscillation of all the metric parameters is stronger for increased feedback level and tends to zero for long external cavities. We also remark that the modulation of the average power does always coexist with the modulation of the repetition rate, amplitude noise and timing jitter (which follow an anti-phase behavior) and could be used as a good and fast qualitative estimation index for predicting the presence and strength of the phenomenon. Therefore, for completeness we also plot in Fig. 7, the modulation depth (or modulation index) of the average power defined as $M = (P_{max} - P_{min})/(P_{max} + P_{min})$ versus the cavity length between 1 and 500 μm for feedback levels of −50, −40 and −30 dB. This confirms as well that stronger feedback intensifies the phenomenon for shorter external cavities but has no impact for longer ones, most likely due to the limited coherence length of the MLL. However, one should consider that although the coherence of the MLLs is very short due to the wide optical bandwidth of the pulses, it is also periodic due to the multimode optical spectrum. Therefore, the consecutive peaks of the laser coherence function should occur at multiples of the laser hot-cavity length $k \cdot L_{las}$ (or time values corresponding to integer multiples of the pulse spacing) and, therefore, we expect a periodical occurrence of the phenomenon at multiples of the laser hot-cavity length. To this end, we simulated the modulation depth of the average power for external cavity lengths around specific peaks of the coherence function, corresponding to macroscopic lengths of $L_{ext} = 0$, 4, 40, 100, 400 mm (k = 0, 10, 25, 100). The results are plotted in Fig. 8a. The ultra-short cavity studied in the previous paragraph corresponds to $k = 0$. It is clearly seen that the power modulation appears on the peaks of the periodic

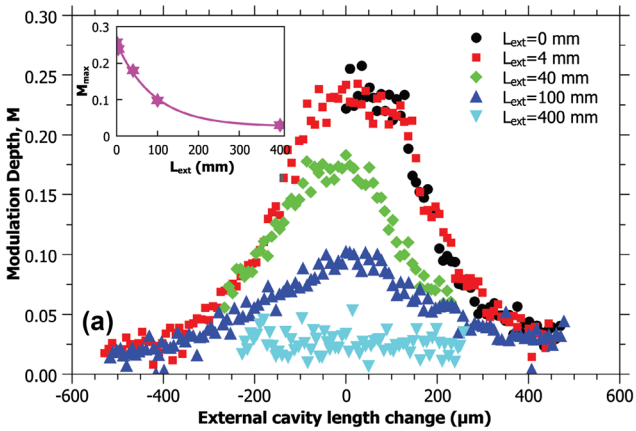

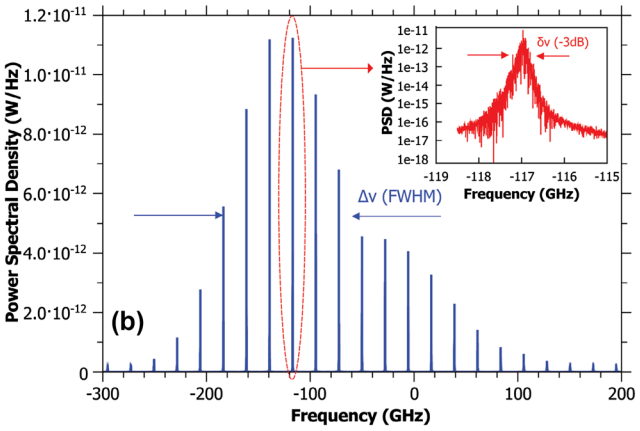

Fig. 8 **a** Modulation depth of the average power versus the variation of the external cavity length around the macroscopic values that correspond to different peaks of the laser coherence function (multiple of the laser cavity $k \cdot L_c$ for k = 0, 1, 10, 25, 100) and a feedback level of −40 dB. The inset shows the maximum modulation depth versus the external cavity length. **b** Optical spectrum of the free running laser in linear scale. The width of the spectrum $\Delta\nu \cong 100$ GHz (FWHM) is reciprocal to the width of each peak of the coherence function (as well as to the ~5 ps pulse duration supposing Gaussian pulses and the well-known formula $\tau = 0.441/\Delta\nu$). The *inset* shows magnified the central mode of the optical spectrum in logarithmic scale for better resolution. The width $\delta\nu$ (−3 dB) of the mode is ~250 MHz and is reciprocal to the overall width of the coherence function (~400 mm) being in good agreement with findings of **a**

coherence function and when the macroscopic length of the external cavity increases the modulation is minimized. This long-term decay is related to the overall width of the coherence function which is the reciprocal of the spectral width of a single longitudinal optical mode of the laser cavity. This is clearly evident in Fig. 8b where the optical spectrum of the laser is shown together with a magnified image of the central optical mode. In conclusion, within the coherence function of the MLL, the wavelength scale oscillation co-exists with the repetition frequency-pulling effect. The latter ultimately predominates the dynamics of the MLL outside the coherence length.

Finally, since the feedback dynamics are known to be strongly dependent on the linewidth enhancement factor (α-factor) of the laser, we investigated the impact of different α-values on the ultra-short delay feedback dynamics of the passively MLL. Figure 9 shows the evolution of the average power, repetition rate, amplitude noise and pulse to pulse jitter for $\alpha = 0.2$ for three characteristic external cavity lengths corresponding to the cases (b)–(d) of Fig. 4 (feedback level is −40 dB, same as in Fig. 4 for comparison). We can see a similar qualitative behavior compared to the $\alpha = 1$ case, but for a quantitative estimation of the impact of α we need a different representation. To this end, we plotted in Fig. 10 the ratio of RIN minima and maxima over the free running value versus the external cavity length for three different α-values $\alpha = 0.2, 1, 2$ assuming a constant feedback strength of −40 dB in the ultra-short

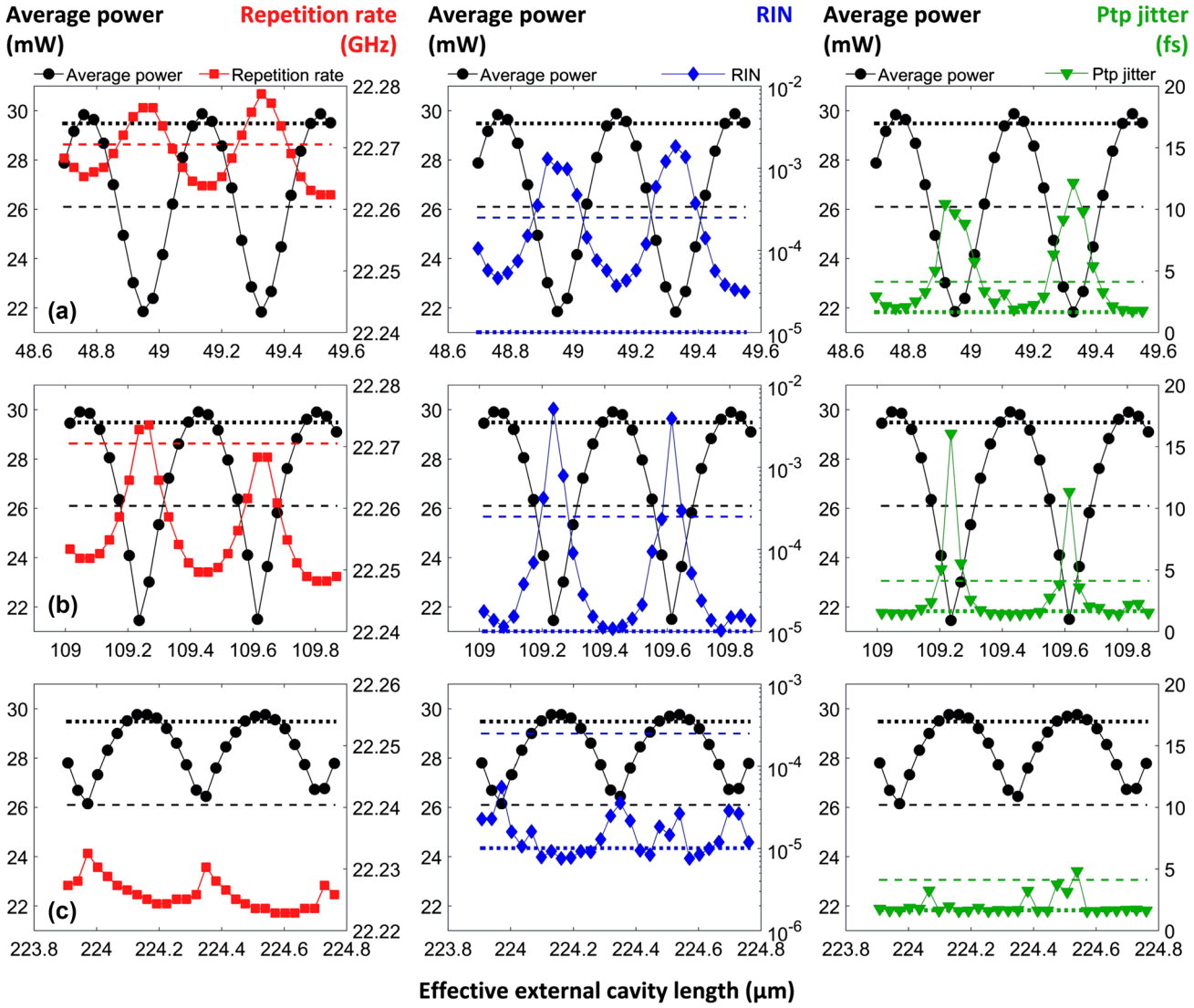

Fig. 9 Repetition rate (*left*), RIN (*center*) and pulse to pulse jitter (*right*) versus nanometric variations of the external cavity around the macroscopic values of 50 μm (*up*), 110 μm (*middle*) and 224 μm (*bottom*) for $\alpha = 0.2$ and a feedback levels of −40 dB. *Dashed* and *dotted lines* show, respectively, the free running and the long cavity values. The evolution of average power is shown for reference in all graphs

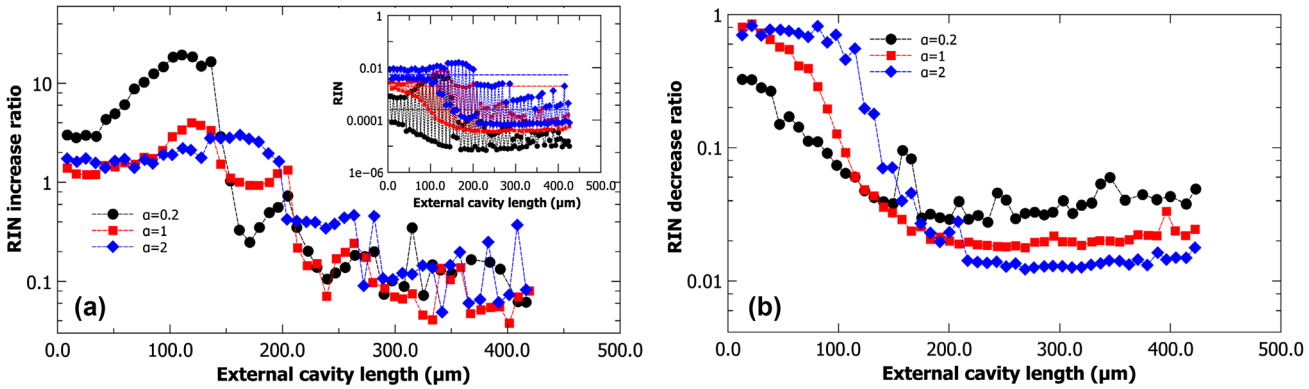

Fig. 10 RIN maxima **a** and minima **b** ratio over the free running value versus the external cavity length for three different α-values. The *inset* shows the RIN evolution versus the external cavity length for the same α-values. *Dashed lines* in the *inset* show the free running RIN values

external cavity case ($k = 0$). It is obvious that the absolute values of RIN scale with α. However, RIN increase ratio under out of phase coherent feedback (expressed as the ratio of the RIN maxima under feedback over the free running RIN value) is larger for lower α-values. For longer cavities (limits of the laser coherence peak), this fades out leading to a similar ratio independently of α, indicating the role of coherence characteristics of the laser. Regarding RIN decrease ratio (expressed as RIN minima over the free running RIN value, see Fig. 10b), one can see that a larger α-value leads to a faster decrease and a lower overall value at the limits of the laser coherence length (although absolute RIN values are larger). A similar behavior has been also observed for the pulse to pulse jitter. Nevertheless, a more rigorous analysis is not obvious here because different α-values lead the laser to different free running noise characteristics. Finally, since only spontaneous emission has been considered as a noise source in our model, the absolute values of noise parameters predicted by our calculations could be different if a more complete noise model is considered.

4 Conclusion

We presented a detailed modeling of the dynamics of a mode-locked semiconductor laser under feedback from an external cavity emphasizing on the analysis of sub-wavelength periodic phenomena. We studied the main performance parameters that fully characterize the operation of an MLL that is the average power, repetition rate, pulse amplitude noise and timing jitter. The obtained results show that the dynamics of the laser exhibit an oscillatory behavior with a $\lambda/2$ periodicity, apparent around integer multiples of the laser cavity, namely for external cavity lengths that coincide with the periodic instances of the laser coherence function. The short-term decay of the phenomenon is in the time scale of the pulse duration, whereas the long-term decay is due to the influence of noise on the emitted pulses and, therefore, it is related (reciprocal) to the width of the spectrum modes. This sub-wavelength phenomenon co-exists and is superimposed on the (microwave periodicity) pulling-related dynamics of the semiconductor MLLs, being dominant for ultra-short external cavities where pulling is weaker. In addition, our results show that a significant change in the MLL performance parameters can be triggered by moderate feedback levels (≥ -50 dB) which is lower than the residual reflection of an anti-reflection coating of a tapered fiber that is used for power collection in a pigtailed laser. By controlling the phase of the induced residual feedback, optimization of the laser performance could be achieved instead of potential degradation by a random feedback phase. Therefore, our study could be useful for the optimization of the semiconductor laser operation in all setups that involve ultra-short external cavity lengths as in integrated designs or in power collection with fiber tapers.

References

1. S. Donati, M.T. Fathi, IEEE J. Quantum Electron. **48**, 1352–1359 (2012)
2. Junji Ohtsubo, *Semiconductor lasers: stability, instability and chaos (optical sciences)* (Springer, New York, 2006)
3. C.-Y. Lin, F. Grillot, Y. Li, R. Raghunathan, L.F. Lester, IEEE J. Sel. Top. Quantum Electron. **17**, 1311–1317 (2011)
4. L. Drzewietzki, S. Breuer, W. Elsäßer, Opt. Express **21**, 16142–16161 (2013)
5. G. Fiol, M. Kleinert, D. Arsenijević, D. Bimberg, Semicond. Sci. Technol. **26**, 014006 (2011)
6. C. Simos, H. Simos, C. Mesaritakis, A. Kapsalis, S. Syvridis, Opt. Commun. **313**, 248–255 (2014)
7. C. Otto, K. Ludge, A.G. Vladimirov, M. Wolfrum, E. Scholl, N. J. Phys. **14**, 113033 (2012)
8. O. Solgaard, K.Y. Lau, IEEE Photon. Technol. Lett. **5**, 1264–1267 (1993)

9. E.A. Avrutin, B.M. Russell, IEEE J. Quantum Electron. **45**, 1456–1464 (2009)
10. H. Simos, C. Simos, C. Mesaritakis, D. Syvridis, IEEE J. Quantum Electron. **48**, 872–877 (2012)
11. T. Heil, I. Fischer, W. Elsäßer, A. Gavrielides, Phys. Rev. Lett. **87**, 243901 (2001)
12. O. Ushakov, S. Bauer, O. Brox, H.-J. Wünsche, F. Henneberger, Phys. Rev. Lett. **92**, 043902 (2004)
13. K. Merghem, C. Calo, V. Panapakkam, A. Martinez, F. Lelarge, A. Ramdane, IEEE J. Sel. Top. Quantum Electron. **21**, 1101407 (2015)
14. P. Spano, S. Piazzolla, M. Tamburini, IEEE J. Quantum Electron. **20**, 350–357 (1984)
15. J. Kitching, R. Boyd, A. Yariv, Y. Shevy, Opt. Lett. **19**, 1331–1333 (1994)
16. J. Kitching, A. Yariv, Y. Shevy, Phys. Rev. Lett. **74**, 3372–3375 (1995)
17. K. Vahala, A. Yariv, Appl. Phys. Lett. **45**, 501–503 (1984)
18. M.A. Newkirk, K.J. Vahala, IEEE J. Quantum Electron. **27**, 13–22 (1991)
19. D. Eliyahu, R.A. Salvatore, A. Yariv, J. Opt. Soc. Am. B **7**, 1619 (1996)
20. R. Paschotta, Appl. Phys. B **79**, 163–173 (2004)
21. H. Simos, C. Simos, C. Mesaritakis, D. Syvridis, IEEE Photon. Technol. Lett. **27**, 506–509 (2015)
22. J. Mulet, J. Mørk, IEEE J. Quantum Electron. **42**(3), 249 (2006)
23. D. von der Linde, Appl. Phys. B **39**, 201–217 (1986)
24. H. Haus, A. Mecozzi, IEEE J. Quantum Electron. **29**, 983–996 (1993)
25. D. Eliyahu, R.A. Salvatore, A. Yariv, J. Opt. Soc. Am. B **14**, 167 (1997)
26. F. Kéfélian, Sh O'Donoghue, M.T. Todaro, J.G. McInerney, G. Huyet, IEEE Photonics Tech. Lett. **20**, 16 (2008)